

## Coherent Diffraction Radiation experiment at CTF3—Simulation studies

K. LEKOMTSEV<sup>(1)(\*)</sup>, G. BLAIR<sup>(1)</sup>, G. BOORMAN<sup>(1)</sup>, R. CORSINI<sup>(2)</sup>,  
P. KARATAEV<sup>(1)</sup>, T. LEFEVRE<sup>(2)</sup> and M. MICHELER<sup>(1)</sup>

<sup>(1)</sup> *John Adams Institute at Royal Holloway University of London  
Egham, Surrey, TW20 0EX, UK*

<sup>(2)</sup> *CERN CH-1211 - Geneva 23, Switzerland*

(ricevuto il 22 Dicembre 2010; pubblicato online il 7 Luglio 2011)

**Summary.** — A two-target model was developed for the simulations of Coherent Diffraction Radiation (CDR) phenomenon for the experiment at the CLIC Test Facility 3 (CTF3 at CERN). The model is based on a classical DR theory. The radiation distribution from the targets, as a function of the angle and the frequency, was calculated for the first and the second target separately in order to understand how the final radiation distribution from the two targets, working as a system, is formed. The final radiation distribution of destructive interference between the two targets was obtained as well. The distributions were calculated for the working parameters of both the CTF3 and the experimental setup and were used for a single-electron spectrum calculation, required for the bunch profile reconstruction.

PACS 41.60.-m – Radiation by moving charges.

### 1. – Introduction

A novel scheme for the drive beam generation has been proposed for the future Compact Linear Collider (CLIC), in which a long bunch train with a low bunch repetition frequency will be accelerated with a low RF frequency. The optimization and monitoring of the longitudinal charge distribution in the bunch is crucial for the optimal performance of the CLIC drive beam as well as for maximization of the luminosity at the CLIC interaction point [1].

Diffraction radiation (DR) is widely used as a tool for transverse [2] and longitudinal [3] beam parameters monitoring. DR arises when a charged beam passes by in the vicinity of a target, the effect of the beam interaction with the target material is minimal and a smaller perturbation to the beam is produced compared with other diagnostics,

(\*) E-mail: [Konstantin.Lekomtsev.2009@live.rhul.ac.uk](mailto:Konstantin.Lekomtsev.2009@live.rhul.ac.uk)

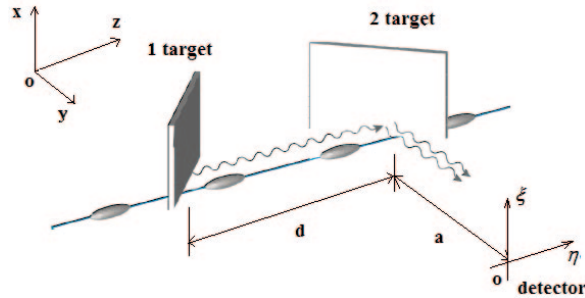


Fig. 1. – Schematic layout of the two-target configuration.

such as Transition Radiation. Coherent Diffraction Radiation (CDR) was suggested as a tool for the beam diagnostics due to its non-invasive nature and utilised in this experiment. The intensity of CDR is defined by the following equation:

$$(1) \quad S(\omega) = S_e(\omega)N^2F(\omega),$$

where  $S(\omega)$  is the measured spectrum,  $S_e(\omega)$  is the single-electron spectrum and it has to be predicted precisely,  $N$  is the number of electrons in the bunch;  $F(\omega)$  (the goal of the measurements) is the bunch form factor and it contains information about the longitudinal distribution of electrons in the bunch.

We proposed the following scheme for the CDR generation as shown in fig. 1. It required in-depth theoretical studies of the two-target configuration. One of the main goals of the two-target configuration is the suppression of the wakefields and the Coherent Synchrotron Radiation backgrounds, traveling with the beam and originated from upstream of the setup. Transverse kick compensation is achieved as well, by positioning the targets at 45 degrees with respect to the beam. In this paper, the current progress on the simulations of the CDR from the two targets and calculation of the single-electron spectrum will be reported. The main parameters used in the simulations are presented in table I.

## 2. – Simulations

**2.1. Backward Diffraction Radiation from the second target.** – For the calculations we shall use a classical theory of Diffraction Radiation (DR), based on Huygens principle of plane wave diffraction. In fact classical DR theory describes backward DR only. However, for a metallic foil and millimetre wavelengths we can use an ideal conductor approximation. In this case BDR characteristics coincide with FDR ones [4]. A particle field is introduced as a superposition of its pseudo-photons and when they are scattered off a target surface, they are converted into the real ones and propagate either in the direction of the specular reflection (BDR) or along the particle trajectory (FDR).

In this subsection we consider the radiation from the second target only, excluding influence of the first target at all. Consider an electron moving along the  $z$ -axis. Each point of the target surface can be represented as an elementary source of the radiation. Two polarization components of the DR can be represented as a superposition of the

TABLE I. – *CTF3 and CDR experiment parameters.*

Beam energy ( $\gamma$ )	235	
Bunch charge	2.3	nC
Bunch spacing frequency	1.5 or 3	GHz
Target dimensions (projected)	$40 \times 40$	mm
Observation wavelength ( $\lambda$ )	5	mm
First target impact parameter ( $h_1$ ) (upper pos.)	30	mm
First target impact parameter (lower pos.)	10	mm
Second target impact parameter ( $h_2$ )	10	mm
Distance between the targets ( $d$ )	0.25	m
Distance from the second target to the obs. plane ( $a$ )	2	m

waves from all elementary sources at a distance  $\mathbf{r}$  from the target [4]:

$$(2) \quad E_r = -\frac{1}{4\pi^2} \iint E'(x_r, y_r) \frac{e^{i\phi}}{r} dx_r dy_r.$$

$E'(x_r, y_r)$  is the amplitude of the radiation source positioned at  $(x_r, y_r)$ ,  $\phi$  defines the phase advance of the photons emitted by each elementary radiation source,  $r$  is the distance from the radiation source at the target to the observation point.

The amplitude  $E'(x_r, y_r)$  can be represented as a Fourier transform of the incident particle field [4]:

$$(3) \quad \begin{aligned} E'(x_r, y_r) &= -\frac{ie}{2\pi^2} \iint \frac{k'_{x,y} \exp[i(k'_x x_r + k'_y y_r)]}{k'^2_x + k'^2_y + k^2 \gamma^{-2}} dk'_x dk'_y \\ &= \frac{ek}{\pi\gamma} \begin{pmatrix} \cos \psi_r \\ \sin \psi_r \end{pmatrix} K_1 \left( \frac{k}{\gamma} \rho_r \right), \end{aligned}$$

where  $k$  is the wave number,  $\lambda$  is the wavelength of the DR,  $\gamma$  is the Lorentz factor,  $k'_{x,y}$  are the components of the electron pseudo-photon wave vector,  $\rho_r$  and  $\psi_r$  are the radius and the azimuthal angle of the particle field in a polar coordinate system and  $K_1$  is the modified Bessel function of the first order.

At the observation plane  $\xi = \rho_r \cos \psi_r$  and  $\eta = \rho_r \sin \psi_r$  are the coordinates in their polar representation. Parameters  $(\xi - x_r)/a$  and  $(\eta - y_r)/a$  determine the angles of the photon emission by the arbitrary elementary source and in ultrarelativistic case they are of order of  $\gamma^{-1}$ .

Therefore, a phase term of the photons propagating from the target to the observation plane can be written as follows [5]:

$$(4) \quad \frac{\exp[ik|\mathbf{r}|]}{|\mathbf{r}|} \approx \frac{\exp[ika]}{a} \exp \left[ \frac{ik}{2a}(x_r^2 + y_r^2) - \frac{ik}{a}(x_r \xi + y_r \eta) + \frac{ik}{2a}(\xi^2 + \eta^2) \right].$$

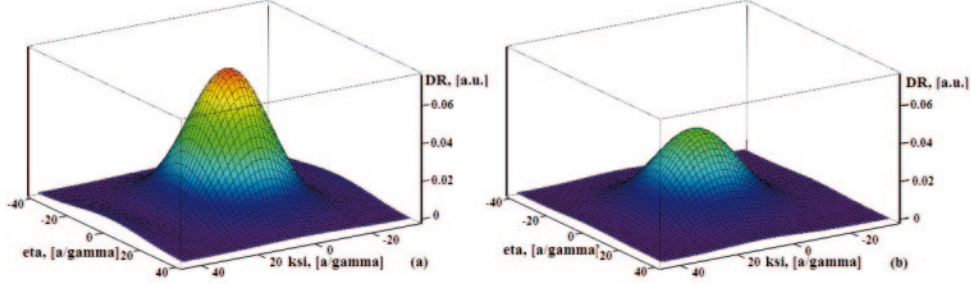


Fig. 2. – (a) The distribution of the Backward Diffraction Radiation from the second target. (b) The distribution of the Forward Diffraction Radiation from the first target, diffracted at the second one.

Consequently two polarization components of the DR from the second target can be written as

$$(5) \quad E_{r_2}^2(\xi, \eta) = -\frac{1}{4\pi^2} \frac{ek}{\pi\gamma} \frac{\exp[ika]}{a} \iint \left( \frac{\frac{x_2}{\sqrt{x_2^2+y_2^2}}}{\frac{y_2}{\sqrt{x_2^2+y_2^2}}} \right) K_1 \left( \frac{k}{\gamma} \sqrt{x_2^2 + y_2^2} \right) \times \exp \left[ \frac{ik}{2a} ((x_2 - \xi)^2 + (y_2 - \eta)^2) \right] dx_2 dy_2,$$

where  $x_2$  and  $y_2$  are the coordinates at the target surface and  $a$  is the distance between the target and the observation plane.

The DR spatial distribution in the general form can be written as

$$(6) \quad \frac{d^2 W^{\text{DR}}}{d\omega d\Omega} = 4\pi^2 k^2 a^2 (|E_x^{\text{DR}}|^2 + |E_y^{\text{DR}}|^2),$$

where  $E_x^{\text{DR}}$  and  $E_y^{\text{DR}}$  are horizontal and vertical polarization components of the DR, respectively.

Substituting eq. (5) into eq. (6) and taking into account that  $e^2/\hbar c = \alpha = 1/137$  we obtain spatial distribution of the BDR from the second target:

$$(7) \quad \frac{d^2 W^{\text{DR}}}{d\omega d\Omega} = \frac{4}{137\lambda^4 \gamma^2} \left[ \iint \left( \frac{\frac{x_2}{\sqrt{x_2^2+y_2^2}}}{\frac{y_2}{\sqrt{x_2^2+y_2^2}}} \right) K_1 \left( \frac{k}{\gamma} \sqrt{x_2^2 + y_2^2} \right) \times \exp \left[ \frac{ik}{2a} ((x_2 - \xi)^2 + (y_2 - \eta)^2) \right] dx_2 dy_2 \right]^2.$$

In fig. 2(a), the graphical result for eq. (7) is presented. The simulations are done for the target positioned in the infinite vacuum space. The BDR distribution at the observation plane is calculated for the parameters shown in table I, it is a single-mode distribution. The detailed analysis of the CDR characteristics for the single target and the CTF3 beam parameters was presented in [6]. Therefore in this paper we shall concentrate on the two-target configuration.

**2.2. Forward Diffraction Radiation from the first target.** – Assuming that for our wavelength and a metallic foil, FDR and BDR are identical, we obtain the FDR from the first target which propagates towards the second target and diffracted from it. The first stage of the process (electric field of the FDR produced at the first target and propagating towards the second one) can be written as

$$(8) \quad E_{r_1}^{1 \rightarrow 2}(x_2, y_2) = -\frac{1}{4\pi^2} \frac{ek}{\pi\gamma} \frac{\exp[ikd]}{d} \iint \left( \frac{\frac{x_1}{\sqrt{x_1^2+y_1^2}}}{\frac{y_1}{\sqrt{x_1^2+y_1^2}}} \right) K_1 \left( \frac{k}{\gamma} \sqrt{x_1^2 + y_1^2} \right) \\ \times \exp \left[ \frac{ik}{2d} ((x_1 - x_2)^2 + (y_1 - y_2)^2) \right] dx_1 dy_1,$$

where  $x_1, y_1$  are the coordinates at the first target surface and  $d$  is the distance between the targets.

Diffraction of the FDR at the second target surface and further propagation of the diffracted radiation towards the observation plane give us the final result. It can be calculated simply by multiplication of eq. (8) by the phase term of the diffracted photons propagating from the second target to the observation plane. The phase term can be written as

$$(9) \quad \frac{\exp[ika]}{a} \exp \left[ \frac{ik}{2a} (x_2^2 + y_2^2) - \frac{ik}{a} (x_2\xi + y_2\eta) + \frac{ik}{2a} (\xi^2 + \eta^2) \right].$$

The final expression for the FDR from the first target is the following:

$$(10) \quad E_{r_1}^1(\xi, \eta) = -\frac{1}{4\pi^2} \frac{ek}{\pi\gamma} \frac{\exp[ik(d+a)]}{ad} \frac{k}{2\pi i} \iiint \left( \frac{\frac{x_1}{\sqrt{x_1^2+y_1^2}}}{\frac{y_1}{\sqrt{x_1^2+y_1^2}}} \right) K_1 \left( \frac{k}{\gamma} \sqrt{x_1^2 + y_1^2} \right) \\ \times \exp \left[ \frac{ik}{2d} ((x_1 - x_2)^2 + (y_1 - y_2)^2) + \frac{ik}{2a} ((x_2 - \xi)^2 + (y_2 - \eta)^2) \right] dx_1 dy_1 dx_2 dy_2.$$

For further calculations we rearrange the terms and replace the integration over  $x_2$  and  $y_2$  with the combination of Fresnel's integrals. This allows us to use a rational approximation of Fresnel's integrals in order to reduce the calculation time and increase performance of the code (see Appendix A). Finally we can obtain the final result for eq. (10):

$$(11) \quad E_{r_1}^1(\xi, \eta) = \frac{ie \exp[ik(a+d)]}{4\pi^2 \lambda \gamma (a+d)} \iint \left( \frac{\frac{x_1}{\sqrt{x_1^2+y_1^2}}}{\frac{y_1}{\sqrt{x_1^2+y_1^2}}} \right) K_1 \left( \frac{k}{\gamma} \sqrt{x_1^2 + y_1^2} \right) \\ \times \left( \left[ \cos \left[ \frac{k}{2(a+d)} ((x_1 - \xi)^2 + (y_1 - \eta)^2) \right] (T_1 T_2 - T_3 T_4) \right. \right. \\ \left. \left. - \left[ \sin \left[ \frac{k}{2(a+d)} ((x_1 - \xi)^2 + (y_1 - \eta)^2) \right] (T_1 T_4 + T_3 T_2) \right] \right. \right. \\ \left. \left. + i \left[ \cos \left[ \frac{k}{2(a+d)} ((x_1 - \xi)^2 + (y_1 - \eta)^2) \right] (T_1 T_4 + T_3 T_2) \right. \right. \right. \\ \left. \left. \left. + \left[ \sin \left[ \frac{k}{2(a+d)} ((x_1 - \xi)^2 + (y_1 - \eta)^2) \right] (T_1 T_2 - T_3 T_4) \right] \right) \right) dx_1 dy_1,$$

where  $T_1 = T_1(x_1, \xi)$ ,  $T_2 = T_2(y_1, \eta)$ ,  $T_3 = T_3(x_1, \xi)$ ,  $T_4 = T_4(y_1, \eta)$  (see appendix B) are the terms containing Fresnel's integrals.

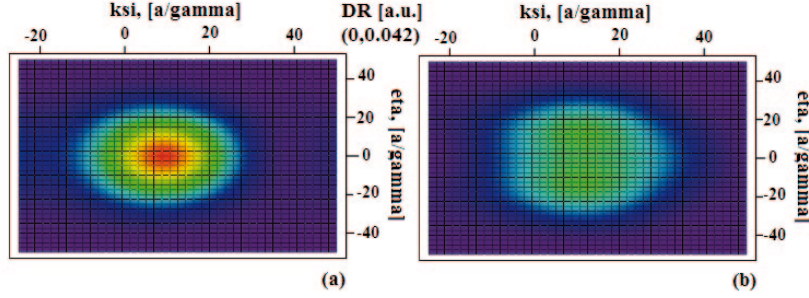


Fig. 3. – The distribution of the Diffraction Radiation from the two targets: (a) the first target is in the upper position (impact parameter  $h_1 = 30$  mm) and the second target is in the lower position (impact parameter  $h_2 = 10$  mm). (b) Both targets are at the same distance from the beam ( $h_1 = h_2 = 10$  mm).

In fig. 2(b), the graphical result for the spatial distribution of the FDR from the first target (eq. (11)) is presented. The targets are positioned at the same distance from the beam ( $h_1 = h_2 = 10$  mm). The FDR is produced at the first target surface and propagates towards the second target and then diffracted from it. In fig. 2(b) we observe single-mode distribution as well as for the second target, however the intensity of the radiation decreases by approximately 30% due to the diffraction losses.

**2.3. Diffraction Radiation from the two targets.** – Once the two radiation components are obtained, we can derive the DR distribution from the two targets. We observe interference between the BDR from the second target and the FDR from the first target, therefore the following formula for the radiation spatial distribution is applied:

$$(12) \quad \frac{d^2 W_r^{\text{DR}}}{d\omega d\Omega} = 4\pi^2 k^2 a^2 \left[ \left( \text{Re } E_{r_1}^1 - \text{Re} \left[ E_{r_2}^2 \exp \left[ \frac{ikd}{\beta} \right] \right] \right)^2 + \left( \text{Im } E_{r_1}^1 - \text{Im} \left[ E_{r_2}^2 \exp \left[ \frac{ikd}{\beta} \right] \right] \right)^2 \right],$$

where  $E_{r_1}^1$  and  $E_{r_2}^2$  are the FDR from the first target and the BDR from the second target correspondingly, calculated in the previous subsections;  $\beta = v/c$  is the speed of an electric charge in terms of the speed of light. The  $\exp[ikd/\beta]$  defines the phase delay due to the particle moving from the first target to the second one.

Figure 3 shows the distributions of the DR from the two targets for two main configurations of the system. When the first (upstream) target is lifted up and its influence on the distribution is suppressed for the given parameters of the setup and the machine, the distribution has a single-mode nature. Once the first target is positioned at the same distance as the second target, the distribution converts itself into the dual-mode one and it is more dispersed and less intensive as well. The latter is the direct consequence of destructive interference.

By integrating the DR distributions over a detector aperture the single-electron spectrum can be obtained. Figure 4 shows the spectra for three different configurations of the system. The intensity of the detected radiation decreases due to the destructive interference when the upstream target is gradually inserted into the beam pipe.

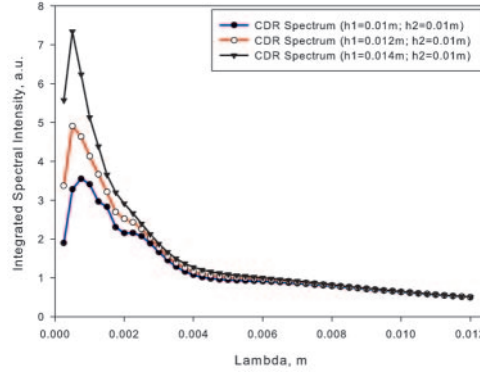


Fig. 4. – The DR spectra for three configurations of the experimental setup. The spectra were calculated for the detector with  $20 \times 20$  mm aperture.

### 3. – Conclusions

Simulation studies for the two-target configuration have been performed. The process of CDR emission was considered in several steps. Simulations were based on the classical theory of Diffraction Radiation. A thin-foil approximation was used, the dimensions of the targets were fixed, the distance between the targets and the observation plane was fixed as well. The ultimate goal of the simulations was to obtain the single-electron spectrum, which can be utilized for longitudinal electron bunch shape reconstruction.

The presented simulations play a crucial role in achieving the optimal configuration of the experimental setup. The suggested two-target configuration allows the background suppression by the first target; the transverse kick compensation, by positioning the targets at 45 degrees with respect to the beam and also the first target works as an additional source of the DR. The model will later be used for the analysis of the experimental data obtained in the network of our collaboration on development of the CDR longitudinal beam profile monitor for CLIC.

APPENDIX A.

#### Fresnel's integrals

We shall consider two types of Fresnel's integrals  $C(z) = \int_0^z \cos(\frac{\pi}{2}t^2)dt$  and  $S(z) = \int_0^z \sin(\frac{\pi}{2}t^2)dt$  and rational approximation for them [7]:

$$(A.1) \quad C(z) = \frac{1}{2} + \frac{1 + 0.926z}{2 + 1.792z + 3.104z^2} \sin\left(\frac{\pi}{2}z^2\right) - \frac{1}{2 + 4.142z + 3.492z^2 + 6.67z^3} \cos\left(\frac{\pi}{2}z^2\right),$$

$$(A.2) \quad S(z) = \frac{1}{2} - \frac{1 + 0.926z}{2 + 1.792z + 3.104z^2} \cos\left(\frac{\pi}{2}z^2\right) - \frac{1}{2 + 4.142z + 3.492z^2 + 6.67z^3} \sin\left(\frac{\pi}{2}z^2\right),$$

the considered Fresnel integrals also follow the rule

$$(A.3) \quad C(z) = \begin{cases} C(z), & \text{if } z > 0, \\ -C(|z|), & \text{otherwise;} \end{cases} \quad S(z) = \begin{cases} S(z), & \text{if } z > 0, \\ -S(|z|), & \text{otherwise.} \end{cases}$$

## APPENDIX B.

### $T_i$ terms

The terms  $T_i$  containing Fresnel integrals can be expressed as

$$(B.1) \quad T_1(x_1, \xi) = C(t_1(x_1, \xi)) - C(t_2(x_1, \xi)),$$

$$T_2(y_1, \eta) = C(t_3(y_1, \eta)) - C(t_4(y_1, \eta));$$

$$(B.2) \quad T_3(x_1, \xi) = S(t_1(x_1, \xi)) - S(t_2(x_1, \xi)),$$

$$T_4(y_1, \eta) = S(t_3(y_1, \eta)) - S(t_4(y_1, \eta));$$

where

$$t_1(x_1, \xi) = \sqrt{\frac{2(a+d)}{\lambda ad}} \left( x_{\text{height}} + \text{impact} - \frac{ad}{a+d} \left( \frac{x_1}{d} + \frac{\xi}{a} \right) \right),$$

$$t_2(x_1, \xi) = \sqrt{\frac{2(a+d)}{\lambda ad}} \left( \text{impact} - \frac{ad}{a+d} \left( \frac{x_1}{d} + \frac{\xi}{a} \right) \right),$$

$$t_3(y_1, \eta) = \sqrt{\frac{2(a+d)}{\lambda ad}} \left( \frac{y_{\text{width}}}{2} - \frac{ad}{a+d} \left( \frac{y_1}{d} + \frac{\eta}{a} \right) \right),$$

$$t_4(y_1, \eta) = \sqrt{\frac{2(a+d)}{\lambda ad}} \left( -\frac{y_{\text{width}}}{2} - \frac{ad}{a+d} \left( \frac{y_1}{d} + \frac{\eta}{a} \right) \right);$$

$x_{\text{height}} + \text{impact}$  and  $\text{impact}$  are the coordinates which correspond to the upper and the lower edges of the target, and  $-y_{\text{width}}/2$  with  $y_{\text{width}}/2$  correspond to the left and the right edges of the target.

\* \* \*

Work supported by the EU under contract PITN-GA-2008-215080.

## REFERENCES

- [1] GESCHONKE G. *et al.*, CTF3 Design report, CERN/PS 2002-08 (2002).
- [2] KARATAEV P. *et al.*, *Phys. Rev. Lett.*, **93** (2004) 244802.
- [3] CASTELLANO M. *et al.*, *Phys. Rev. E.*, **63** (2001) 056501.
- [4] TER-MIKAELYAN M. L. *et al.*, *High Energy Electromagnetic Processes in Condensed Media* (Wiley-Interscience, New York) 1972.
- [5] KARATAEV P., *Phys. Lett. A*, **345** (2005) 428.
- [6] MICHELER M. *et al.*, *J. Phys.: Conf. Ser.*, **236** (2010) 012021.
- [7] BREZINSKI C. and REDIVO ZAGLIA M., *Extrapolation Methods Theory and Practice* (Elsevier, the Netherlands) 1991.